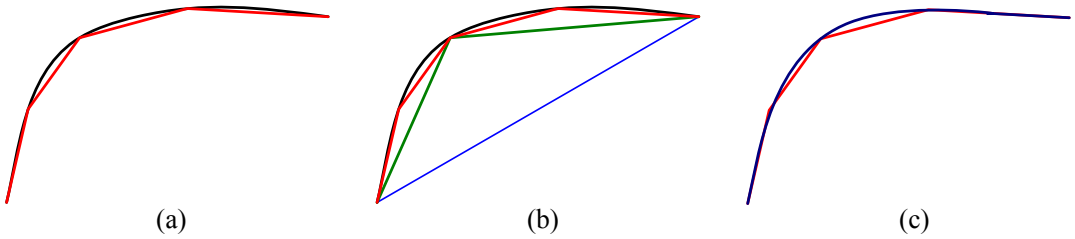

Figure 4.40 Approximating a curve (shown in black) as a polyline or B-spline: (a) original curve and a polyline approximation shown in red; (b) successive approximation by recursively finding points furthest away from the current approximation; (c) smooth interpolating spline, shown in dark blue, fit to the polyline vertices.

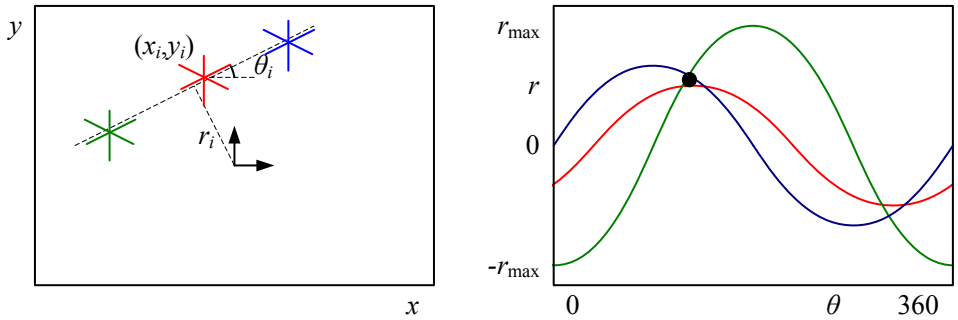

Figure 4.41 Original Hough transform: (a) each point votes for a complete family of potential lines $r_i(\theta) = x_i \cos\theta + y_i \sin\theta$; (b) each pencil of lines sweeps out a sinusoid in (r, θ); their intersection provides the desired line equation.

the point furthest away from the line joining the two endpoints (or the current coarse polyline approximation), as shown in Figure 4.40. Hershberger and Snoeyink (1992) provide a more efficient implementation and also cite some of the other related work in this area.

Once the line simplification has been computed, it can be used to approximate the original curve. If a smoother representation or visualization is desired, either approximating or interpolating splines or curves can be used (Sections 3.5.1 and 5.1.1) (Szeliski and Ito 1986; Bartels, Beatty, and Barsky 1987; Farin 1996), as shown in Figure 4.40c.

4.3.2 Hough transforms

While curve approximation with polylines can often lead to successful line extraction, lines in the real world are sometimes broken up into disconnected components or made up of many collinear line segments. In many cases, it is desirable to group such collinear segments into extended lines. At a further processing stage (described in Section 4.3.3), we can then group such lines into collections with common vanishing points.

The Hough transform, named after its original inventor (Hough 1962), is a well-known technique for having edges "vote" for plausible line locations (Duda and Hart 1972; Ballard 1981; Illingworth and Kittler 1988). In its original formulation (Figure 4.41), each edge point votes for *all* possible lines passing through it, and lines corresponding to high *accumulator* or

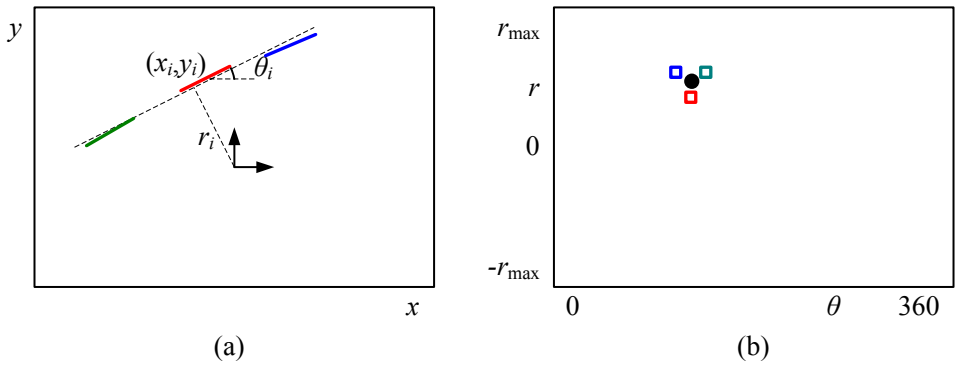

Figure 4.42 Oriented Hough transform: (a) an edgel re-parameterized in polar (r, θ) coordinates, with $\hat{\boldsymbol{n}}_i = (\cos\theta_i, \sin\theta_i)$ and $r_i = \hat{\boldsymbol{n}}_i \cdot \boldsymbol{x}_i$; (b) (r, θ) accumulator array, showing the votes for the three edgels marked in red, green, and blue.

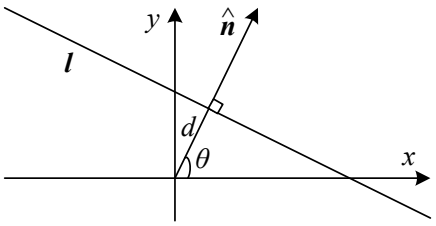

Figure 4.43 2D line equation expressed in terms of the normal $\hat{\boldsymbol{n}}$ and distance to the origin d.

bin values are examined for potential line fits.[9] Unless the points on a line are truly punctate, a better approach (in my experience) is to use the local orientation information at each edgel to vote for a *single* accumulator cell (Figure 4.42), as described below. A hybrid strategy, where each edgel votes for a number of possible orientation or location pairs centered around the estimate orientation, may be desirable in some cases.

Before we can vote for line hypotheses, we must first choose a suitable representation. Figure 4.43 (copied from Figure 2.2a) shows the normal-distance $(\hat{\boldsymbol{n}}, d)$ parameterization for a line. Since lines are made up of edge segments, we adopt the convention that the line normal $\hat{\boldsymbol{n}}$ points in the same direction (i.e., has the same sign) as the image gradient $\boldsymbol{J}(\boldsymbol{x}) = \nabla I(\boldsymbol{x})$ (4.19). To obtain a minimal two-parameter representation for lines, we convert the normal vector into an angle

$$\theta = \tan^{-1} n_y / n_x, \tag{4.26}$$

as shown in Figure 4.43. The range of possible (θ, d) values is $[-180°, 180°] \times [-\sqrt{2}, \sqrt{2}]$, assuming that we are using normalized pixel coordinates (2.61) that lie in $[-1, 1]$. The number of bins to use along each axis depends on the accuracy of the position and orientation estimate available at each edgel and the expected line density, and is best set experimentally with some test runs on sample imagery.

Given the line parameterization, the Hough transform proceeds as shown in Algorithm 4.2.

[9] The Hough transform can also be *generalized* to look for other geometric features such as circles (Ballard 1981), but we do not cover such extensions in this book.

procedure *Hough*$(\{(x, y, \theta)\})$:

1. Clear the accumulator array.
2. For each detected edgel at location (x, y) and orientation $\theta = \tan^{-1} n_y/n_x$, compute the value of
$$d = x\, n_x + y\, n_y$$
and increment the accumulator corresponding to (θ, d).
3. Find the peaks in the accumulator corresponding to lines.
4. Optionally re-fit the lines to the constituent edgels.

Algorithm 4.2 Outline of a Hough transform algorithm based on oriented edge segments.

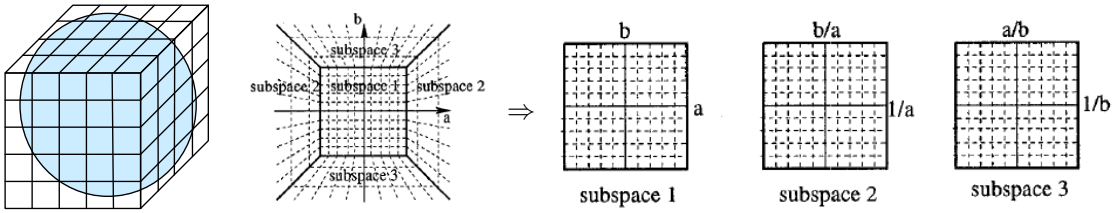

(a) (b)

Figure 4.44 Cube map representation for line equations and vanishing points: (a) a cube map surrounding the unit sphere; (b) projecting the half-cube onto three subspaces (Tuytelaars, Van Gool, and Proesmans 1997) © 1997 IEEE.

Note that the original formulation of the Hough transform, which assumed no knowledge of the edgel orientation θ, has an additional loop inside Step 2 that iterates over all possible values of θ and increments a whole series of accumulators.

There are a lot of details in getting the Hough transform to work well, but these are best worked out by writing an implementation and testing it out on sample data. Exercise 4.12 describes some of these steps in more detail, including using edge segment lengths or strengths during the voting process, keeping a list of constituent edgels in the accumulator array for easier post-processing, and optionally combining edges of different "polarity" into the same line segments.

An alternative to the 2D polar (θ, d) representation for lines is to use the full 3D $\boldsymbol{m} = (\hat{\boldsymbol{n}}, d)$ line equation, projected onto the unit sphere. While the sphere can be parameterized using spherical coordinates (2.8),

$$\hat{\boldsymbol{m}} = (\cos\theta\cos\phi, \sin\theta\cos\phi, \sin\phi), \tag{4.27}$$

this does not uniformly sample the sphere and still requires the use of trigonometry.

An alternative representation can be obtained by using a *cube map*, i.e., projecting $\boldsymbol{m}$ onto the face of a unit cube (Figure 4.44a). To compute the cube map coordinate of a 3D vector $\boldsymbol{m}$, first find the largest (absolute value) component of $\boldsymbol{m}$, i.e., $m = \pm\max(|n_x|, |n_y|, |d|)$,

and use this to select one of the six cube faces. Divide the remaining two coordinates by m and use these as indices into the cube face. While this avoids the use of trigonometry, it does require some decision logic.

One advantage of using the cube map, first pointed out by Tuytelaars, Van Gool, and Proesmans (1997), is that all of the lines passing through a point correspond to line segments on the cube faces, which is useful if the original (full voting) variant of the Hough transform is being used. In their work, they represent the line equation as $ax + b + y = 0$, which does not treat the x and y axes symmetrically. Note that if we restrict $d \geq 0$ by ignoring the polarity of the edge orientation (gradient sign), we can use a half-cube instead, which can be represented using only three cube faces, as shown in Figure 4.44b (Tuytelaars, Van Gool, and Proesmans 1997).

RANSAC-based line detection. Another alternative to the Hough transform is the RANdom SAmple Consensus (RANSAC) algorithm described in more detail in Section 6.1.4. In brief, RANSAC randomly chooses pairs of edgels to form a line hypothesis and then tests how many other edgels fall onto this line. (If the edge orientations are accurate enough, a single edgel can produce this hypothesis.) Lines with sufficiently large numbers of *inliers* (matching edgels) are then selected as the desired line segments.

An advantage of RANSAC is that no accumulator array is needed and so the algorithm can be more space efficient and potentially less prone to the choice of bin size. The disadvantage is that many more hypotheses may need to be generated and tested than those obtained by finding peaks in the accumulator array.

In general, there is no clear consensus on which line estimation technique performs best. It is therefore a good idea to think carefully about the problem at hand and to implement several approaches (successive approximation, Hough, and RANSAC) to determine the one that works best for your application.

4.3.3 Vanishing points

In many scenes, structurally important lines have the same vanishing point because they are parallel in 3D. Examples of such lines are horizontal and vertical building edges, zebra crossings, railway tracks, the edges of furniture such as tables and dressers, and of course, the ubiquitous calibration pattern (Figure 4.45). Finding the vanishing points common to such line sets can help refine their position in the image and, in certain cases, help determine the intrinsic and extrinsic orientation of the camera (Section 6.3.2).

Over the years, a large number of techniques have been developed for finding vanishing points, including (Quan and Mohr 1989; Collins and Weiss 1990; Brillaut-O'Mahoney 1991; McLean and Kotturi 1995; Becker and Bove 1995; Shufelt 1999; Tuytelaars, Van Gool, and Proesmans 1997; Schaffalitzky and Zisserman 2000; Antone and Teller 2002; Rother 2002; Košecká and Zhang 2005; Pflugfelder 2008; Tardif 2009)—see some of the more recent papers for additional references. In this section, we present a simple Hough technique based on having line pairs vote for potential vanishing point locations, followed by a robust least squares fitting stage. For alternative approaches, please see some of the more recent papers listed above.

The first stage in my vanishing point detection algorithm uses a Hough transform to accumulate votes for likely vanishing point candidates. As with line fitting, one possible approach